Report

Human Bone Marrow Mesenchymal Stem Cells Regulate Biased DNA Segregation in Response to Cell Adhesion Asymmetry

Delphine Freida,[1,2,3,4,5,6] Severine Lecourt,[4,5,6] Audrey Cras,[4,5,6] Valérie Vanneaux,[4,5,6] Gaelle Letort,[1,2,7,8]
Xavier Gidrol,[1,2,3] Laurent Guyon,[1,2,3] Jerome Larghero,[4,5,6,9,*] and Manuel Thery[1,2,7,8,9,*]
[1]CEA, Institut de Recherches en Technologies et Sciences pour le Vivant, 17 Rue des Martyrs, 38054 Grenoble, France
[2]University Grenoble-Alpes, F-38041 Grenoble, France
[3]INSERM, U1038, F-38054 Grenoble, France
[4]AP-HP, Hôpital Saint Louis, Unité de Thérapie Cellulaire et Centre d'Investigation Clinique en Biothérapies (CBT501), F-75475 Paris, France
[5]Université Paris Diderot, Sorbonne Paris Cité, F-75475 Paris, France
[6]INSERM, UMRS940, Institut Universitaire d'Hématologie, Hôpital Saint-Louis, F-75475 Paris, France
[7]INRA, USC1359, F-38054 Grenoble, France
[8]CNRS, UMR5168, F-38054 Grenoble France
[9]These authors contributed equally to this work
*Correspondence: jerome.larghero@sls.aphp.fr (J.L.), manuel.thery@cea.fr (M.T.)
http://dx.doi.org/10.1016/j.celrep.2013.09.019

SUMMARY

Biased DNA segregation is a mitotic event in which the chromatids carrying the original template DNA strands and those carrying the template copies are not segregated randomly into the two daughter cells. Biased segregation has been observed in several cell types, but not in human mesenchymal stem cells (hMSCs), and the factors affecting this bias have yet to be identified. Here, we have investigated cell adhesion geometries as a potential parameter by plating hMSCs from healthy donors on fibronectin-coated micropatterns. On symmetric micropatterns, the segregation of sister chromatids to the daughter cells appeared random. In contrast, on asymmetric micropatterns, the segregation was biased. This sensitivity to asymmetric extracellular cues was reproducible in cells from all donors but was not observed in human skin-derived fibroblasts or in a fibroblastic cell line used as controls. We conclude that the asymmetry of cell adhesion is a major factor in the regulation of biased DNA segregation in hMSCs.

INTRODUCTION

A doubled-strand DNA molecule forms the core of a chromosome. One of these strands has served as a template for the assembly of the copy. During S phase and mitosis, strands are separated and duplicated, and then the two resulting chromosomes are spatially segregated. One daughter cell will inherit the chromosome carrying the template strand and the other the copy strand. According to the biased DNA segregation hypothesis, most or all of the chromosomes carrying the original template strand will be segregated into only one of the two daughter cells (Tajbakhsh and Gonzalez, 2009). Biased DNA segregation has been proposed to affect the distribution of epigenetic marks and therefore the differential gene expression between daughter cells (Evano and Tajbakhsh, 2013). Indeed, biased DNA segregation has been shown to regulate asymmetric stem cell fate (Rocheteau et al., 2012).

Biased DNA segregation has been documented in various species ranging from bacteria to mammals, most generally in the context of asymmetric stem cell divisions (Tajbakhsh and Gonzalez, 2009). It has been observed both in vivo and in vitro in several mammalian progenitor or stem cell types for striated muscle (Shinin et al., 2006), mammary gland (Smith, 2005), colon (Falconer et al., 2010), intestine (Potten et al., 2002), cardiac muscle (Kajstura et al., 2012), and neurons (Karpowicz et al., 2005). However, the absence of biased DNA segregation in various types of stem cells (Kiel et al., 2007; Sotiropoulou et al., 2008; Escobar et al., 2011) and its occurrence in tumor-derived or immortalized cells (Merok et al., 2002; Pine et al., 2010) have fueled the debate on the relationship among stemness, asymmetric division, and biased DNA segregation.

Biased DNA segregation has been explored experimentally in a variety of ways, but each of the different procedures used have specific limitations (Tajbakhsh and Gonzalez, 2009). Cell division cannot be monitored directly in vivo; the clear identification of all daughter cells and the detection of rare events are hampered when using fixed tissues (Falconer et al., 2010). Cell division can be video-recorded in vitro, but the critical regulation that the in vivo microenvironment would potentially have on the division of stem cells is excluded (Marthiens et al., 2010; Chen et al., 2013). Finally, both in vivo and in vitro, it can be challenging to distinguish between random and biased DNA segregation

(Falconer et al., 2010). Hence, one way to reconcile conflicting observations on the occurrence of biased DNA segregation is to identify the underlying mechanism and the parameters that regulate the process. However, the mechanism and regulatory parameter remain to be defined (Maiato and Barral, 2013).

In the stem cell niche, stem cell interactions with neighboring cells and with the surrounding extracellular matrix (ECM) regulate their fate (Marthiens et al., 2010; Chen et al., 2013). Adhesion to ECM provides both biochemical and physical signals to stem cells (Rozario and DeSimone, 2010; Brizzi et al., 2012). The spatial distribution of cell adhesion is a key physical signal, in addition to mechanical stimulation (Guilak et al., 2009). It not only defines cell shape but also provides directional cues during asymmetric cell division. Adhesion asymmetry is a fundamental characteristic of asymmetric division (Ellis and Tanentzapf, 2010; Yamashita, 2010). Differences in spatial distribution of the cell's adhesions biases the spontaneous polarization of actin and microtubule networks in interphase (Li and Gundersen, 2008). Further interplay between the actin network and dynamic microtubules leads to metaphase spindle off-centering toward the adhesion-associated cues during cell division (Gönczy, 2008). The consequential asymmetric positioning of the cytokinetic plane generates daughter cells of unequal sizes and unequal contents of adhesion-associated cues, which further determines their distinct fates (Morin and Bellaïche, 2011; Inaba and Yamashita, 2012). We hypothesize that segregation of template and newly synthesized DNA strands can be directed by cell adhesion asymmetry as well and contribute to distinct cell fate determination. To test this hypothesis, we have used surface micropatterning to control the spatial distribution of cell-ECM adhesion and examine biased DNA segregation in primary human mesenchymal stem cells (hMSCs).

RESULTS

Asymmetric Metaphase Plate Position during Mitosis in Response to Adhesion Anisotropy

Modulation of HeLa cell adhesion to ECM with substrate micropatterning has revealed that a slight accumulation in adhesion along one side of the cell is sufficient to induce asymmetric spindle orientation with one of the spindle poles in proximity of the major adhesion-associated cue (Théry et al., 2007). Hence, we first tested the affect of asymmetric distribution of fibronectin on the symmetry of mitotic spindle positioning in hMSCs. hMSCs were isolated from human bone marrow (see Experimental Procedures) and characterized as previously described (Arnulf et al., 2007). To increase the proportion of cells that undergo mitosis during the observation period (<50% cells divide during 40 hr), hMSCs were blocked in early S phase with 1 mM of thymidine for 24 hr. After block release by thymidine washout, and just before entry into mitosis, cells were trypsinized and plated on ECM micropatterns. Elongated micropattern geometries were designed to guide cell division and daughter cell positioning along the mother cell's long axis (Théry et al., 2005). Dumbbell-shaped micropatterns were designed to provide two large and symmetric adhesion areas at the cell extremities (Figure 1A). To provide an asymmetric adhesion geometry and to reduce cell adhesion on one side of the cell without changing the cell's

overall shape, one of the two large adhesive areas of the dumbbell shape was substituted by a Y shape (Figure 1A). Cells were fixed 12 hr after block release (Figure 1).

Actin and microtubule networks appeared asymmetrically organized on asymmetric micropatterns, which is a sign of stably polarized cell (Li and Gundersen, 2008). The microtubule network was more concentrated above the large adhesive area and the actin network formed radial and small concentric arcs of actin fibers. Above the smaller Y-shaped adhesive area, the microtubule network was less concentrated and the actin network formed peripheral stress fibers (Figure 1Aii). Mitotic cells also appeared polarized on asymmetric micropatterns, with asymmetric tear-drop-like shapes, and were off-centered toward the large adhesive area (Figure 1Bii). Cell division asymmetry was also visible during telophase and cytokinesis. Daughter cells seemed to have unequal size and distinct microtubule organizations on asymmetric micropatterns (Figures 1Cii and 1Dii). In contrast, cell division on symmetric micropatterns appeared quite symmetric with respect to all of the above criteria (Figures 1Ai, 1Bi, 1Ci, and 1Di).

The observations made on fixed cells were confirmed with live-cell video recording during which rare mitotic events were easier to capture and quantify. Cell divisions were monitored during 20 hr using phase contrast video microscopy (Figure S1). Chromosome alignment along the metaphase plate was visible in phase contrast. On both symmetric and asymmetric micropatterns, metaphase plates were oriented orthogonally to the long cell axis (Figure S1). This corresponded to an asymmetric orientation on asymmetric micropatterns because the two spindle poles were in proximity of parts of the cell cortex that were not symmetrical. In addition, as previously observed, the metaphase plate was off-centered toward the large adhesive area on the asymmetric micropattern (95% confidence interval [CI] was between 3.6 and 9.7 μm away from the center) and centered on symmetric micropatterns (95% CI was between −4.7 and 1.6 μm around the center) (Figure 1E). Thus, spindle positioning on asymmetric micropatterns displayed most of the typical features associated with asymmetric cell division (Morin and Bellaïche, 2011; Inaba and Yamashita, 2012).

Asymmetric Adhesive Microenvironments Promote Asymmetric Chromatid Segregation in hMSCs

We then tested whether asymmetric spindle position affected DNA segregation. A short pulsed EdU exposure was used to label a single chromatid of a chromatid pair and observe its spatial segregation from the unlabeled chromatid (Figure 2). hMSCs were synchronized in S phase and exposed to 1 μM EdU for 9 hr. To follow the fate of the labeled strands, cells were fixed and immunostained. The partition of labeled strands was estimated by measuring the relative EdU fluorescence intensity in the two daughter cells (Figure S2). After the first division following the pulsed EdU labeling, the daughter cells displayed similar levels of fluorescence in all conditions tested, because, as expected, all chromosomes carried an EdU-labeled DNA strand (Figure S3). Although the sister chromatid segregation was expected to be symmetric, the proportions of labeled DNA between the two daughter cells were not all 50:50 and were as much as 55:45 (Figure S3). This 10% margin of error was
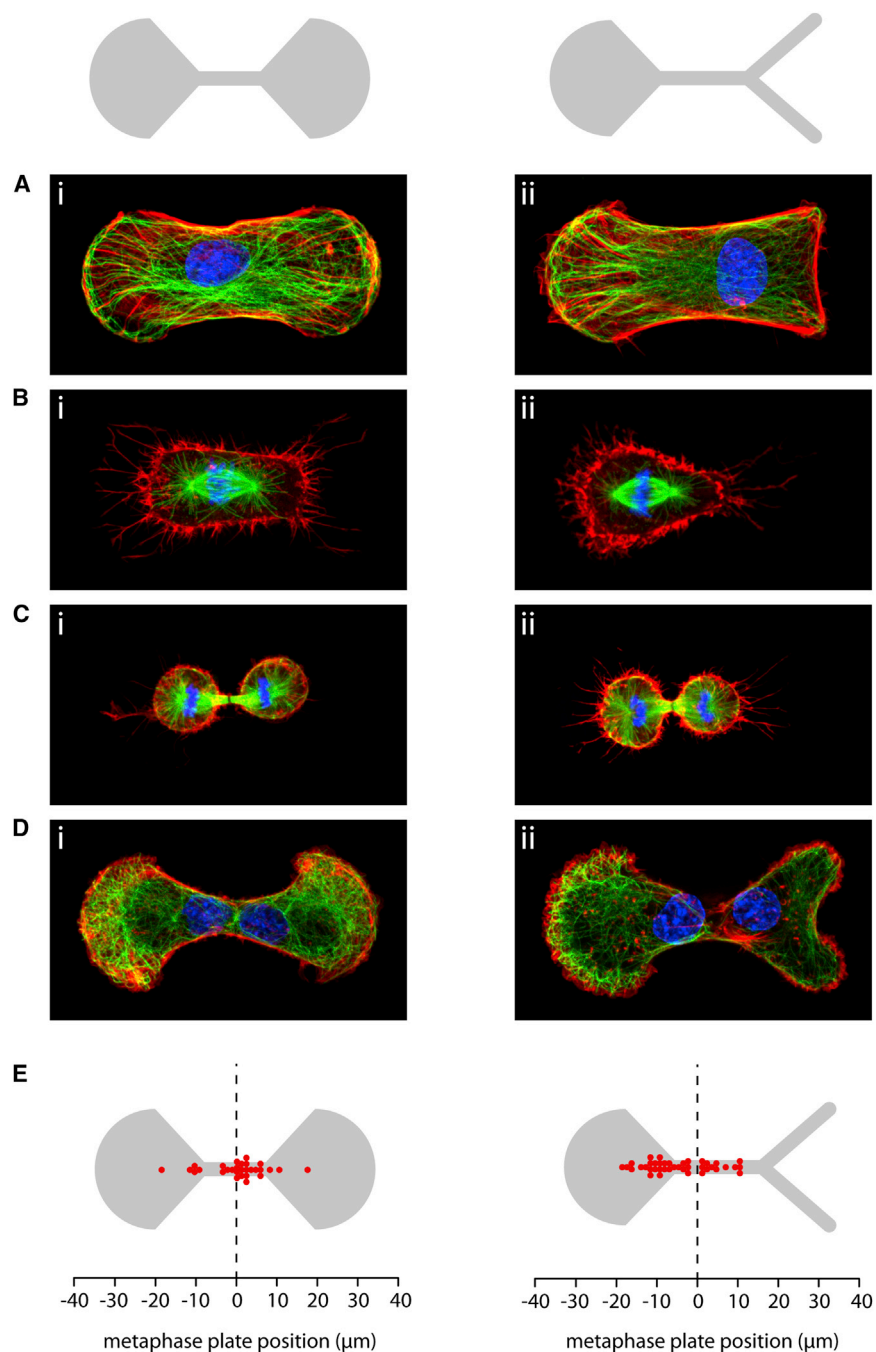
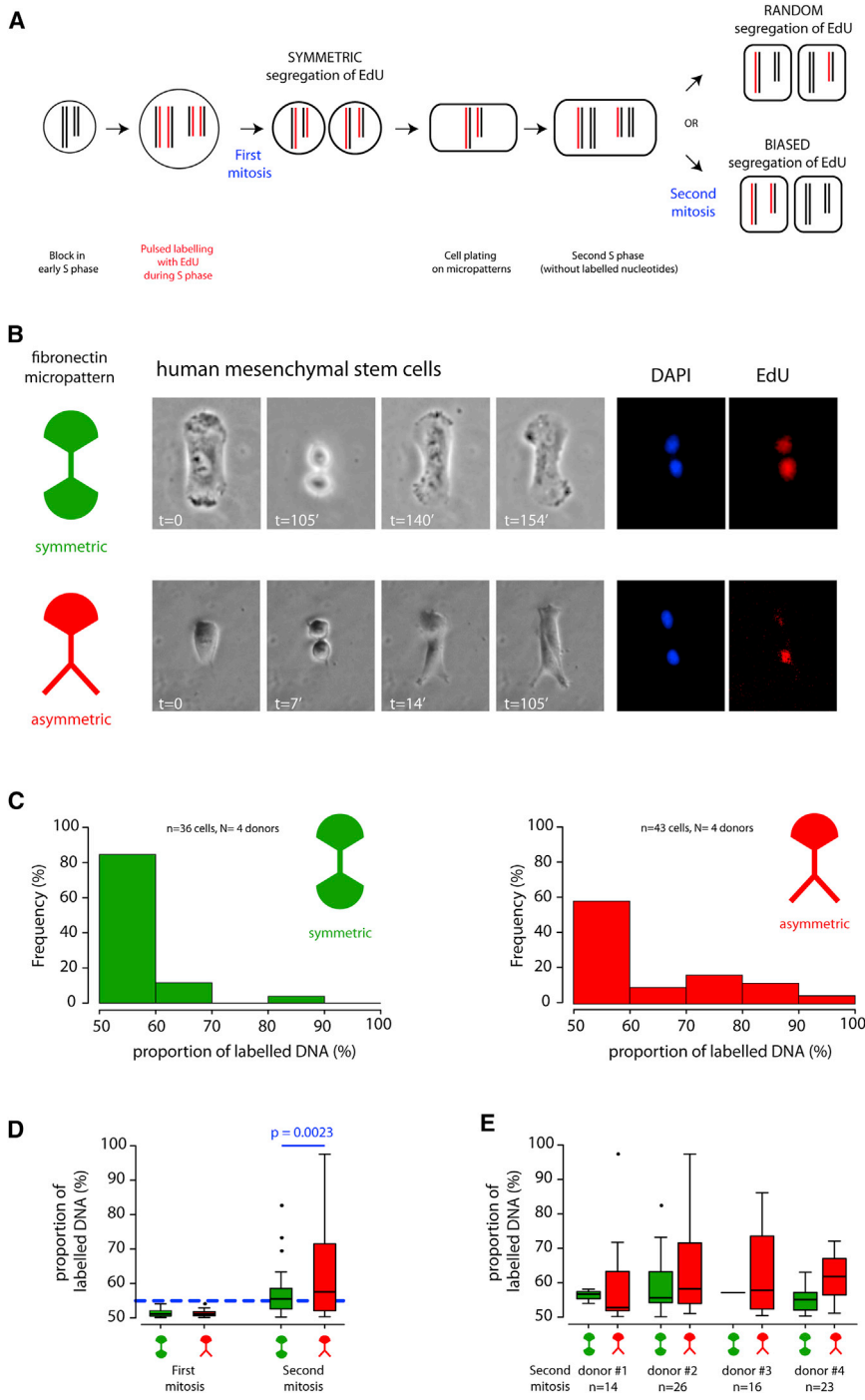**Figure 1. hMSC Division on Fibronectin Micropatterns**

(A–D) Primary cultures of hMSCs were plated on symmetric (i) and asymmetric (ii) fibronectin micropatterns (gray drawings above images). Cells were fixed and stained for actin (red) and tubulin (green). Images show cells in interphase (A), metaphase (B), telophase (C), and cytokinesis (D). (E) Metaphase plate positions were manually measured with respect to the underlying micropattern on phase contrast movies (see Figure S1). Each red dot corresponds to the longitudinal position of a metaphase plate.

matid. Prior to this division, cells were plated on ECM-micropatterns to test the role of cell adhesion on this chromosome segregation. Cell divisions were monitored in video microscopy to ensure that cell doublets actually corresponded to daughter cells (Figure 2B). The low rate of division in these cells was overcome by monitoring a thousand of individual cells in parallel for each donor sample. After the observation period, cells were fixed and stained. About 10% of cells divide during the 20 hr observation period and only about 20% were labeled during the EdU pulse, which corresponded to a dozen of positive cell divisions among a thousand individual cells monitored on the micropatterns. By comparing the fluorescence of the two daughter cells, we could indirectly measure the proportion of DNA carrying the parental, unlabeled strand and neo-synthesized, labeled strand in each cell (Figures 2B and S2). In Figure 2 and in the following, we report the proportion of labeled DNA in the most fluorescent daughter cell, which ranged from 50% (symmetric segregation of labeled DNA) to 100% (asymmetric segregation with all labeled strands in one of the daughter). Asymmetric DNA segregation was observed on both symmetric and asymmetric micropatterns. However, it seemed more frequent on asymmetric micropatterns (Figure 2C). Because the margin of error for symmetric DNA segregation was 10% (Figure S3), only values above 55% were considered as asymmetric DNA segregation (see blue dashed line in Figure 2D). The distributions of asymmetric DNA segregation rates on symmetric and asymmetric micropatterns were significantly different (Wilcoxon test) and the degree of asymmetric DNA segregation was significantly higher on asymmetric micropatterns (Figure 2D). The same tendency was observed in cells obtained from each of the four healthy donors (Figure 2E).

probably due to the limitations of our quantification method due to 3D chromosome organization and nonlinear relationship between DNA staining and the fluorescent signal. However, as illustrated below, the precision for quantifying labeled DNA was sufficient to identify asymmetric segregation.

During the second division, the labeled and unlabeled strands were separated during DNA replication and incorporated into distinct sister chromatids (Figure 2A). So for each chromosome, daughter cells inherited either the labeled or the unlabeled chro-

Figure 2. Quantification of DNA Segregation Asymmetry in hMSCs

(A) Pulsed EdU labeling and chromatid segregation. Chromosomes are represented as two bars corresponding to the two chromatids. Red bars correspond to EdU labeled chromatids. In the case of random DNA segregation, daughters receive a similar amount of labeled DNA strands. In the case of biased DNA, one of the two daughters receives most, if not all, labeled strands.

(B) Primary cultures of hMSCs were plated on symmetric (upper panel) and asymmetric (lower panel) fibronectin micropatterns. Cell divisions were monitored using phase contrast microscopy over 20 hr and further examined after fixation. Cells were immunostained to reveal DNA with DAPI (blue) and the DNA strands that had incorporated EdU (red).

(C) EdU staining was measured in both cells. Histograms show the frequency distribution of the EdU proportion in the more fluorescent daughter (i.e., the DNA segregation rate; between 50% and 100% in 10% intervals) when plated on symmetric (left) and asymmetric (right) micropatterns.

(D) Box plot representations of the distributions of after the first, symmetric mitosis and second mitosis (same data set as in C). Asymmetric DNA segregation rates were defined as rates superior to the threshold of 55% (blue dotted line) defined by the highest DNA segregation rate observed after the first mitosis. Asymmetric DNA segregation rates after the second mitosis were compared with a Wilcoxon test.

(E) Box plot representations of the distributions of DNA segregation rates on symmetric and asymmetric micropatterns for each of the four donors that contributed to the pooled data in (C) and (D).

Asymmetric Adhesive Microenvironments Bias Chromatid Segregation in hMSCs

Numerical simulations were used to explore whether asymmetric DNA segregation was due to a random process or a bias process. The probability distribution defined by the random segregation of 46 pairs of chromatids showed that all DNA segregation rates, although not equally frequent, are possible (see Supplemental Experimental Procedures). Hence, from this simulation, only less than 0.6% of divided cells had asymmetric DNA segregation rates superior to 70% (Figure 3A). Therefore, 70% was set as a reasonable limit above which DNA segregation rates were considered as biased and not due to a random process. Noteworthy, longer chromosome could give a greater contribution to the EdU signal than a shorter one and impinge on fluorescence ratios. We performed similar simulations by taking into account the specific chromosome sizes and found that although the probability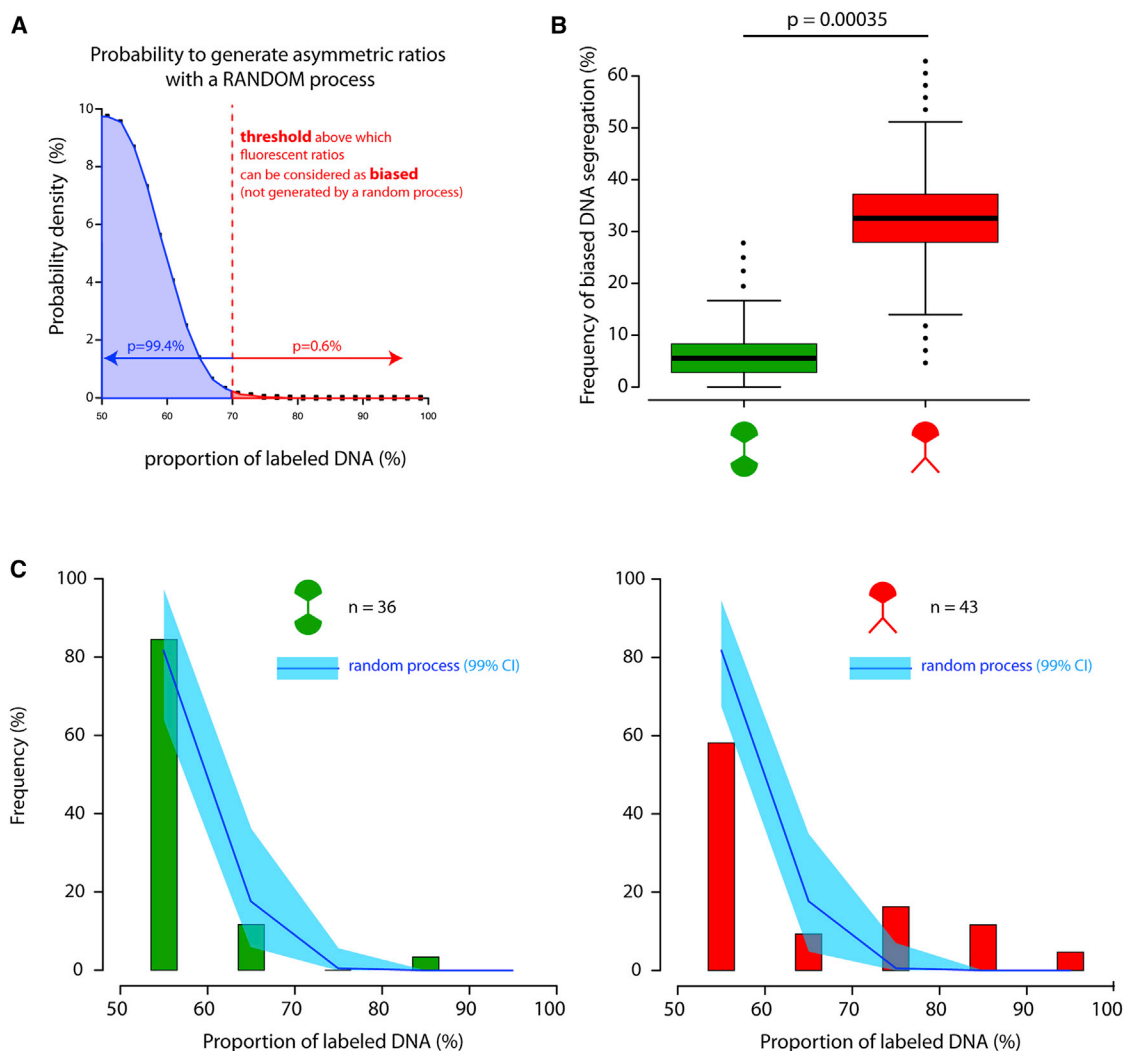 distribution was slightly changed, the probability to observe asymmetric DNA segregation rates superior to 70% was not affected (Figure S4). Therefore, this threshold was used to further analyze the distributions of DNA segregation on symmetric and asymmetric micropatterns.

On symmetric micropatterns, biased DNA segregation was observed in only 2 out of 36 divided hMSCs. Similar frequencies of divided cells were observed when the cells were plated on homogeneously adhesive substrata. In contrast and on asymmetric

Figure 3. Quantification of DNA Segregation Bias in hMSCs

(A) Numerical simulation of the probability distribution defined by the random, unbiased segregation of 46 pairs of chromatids. According to this random process, only 0.6% of the observations (red) would give DNA segregation rates > 70%. Hence, a DNA segregation rate > 70% was considered biased DNA segregation.
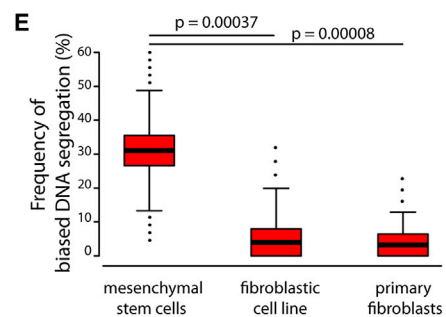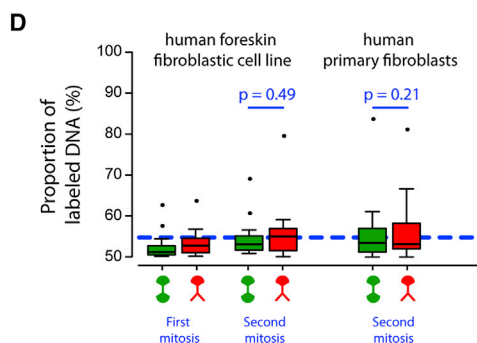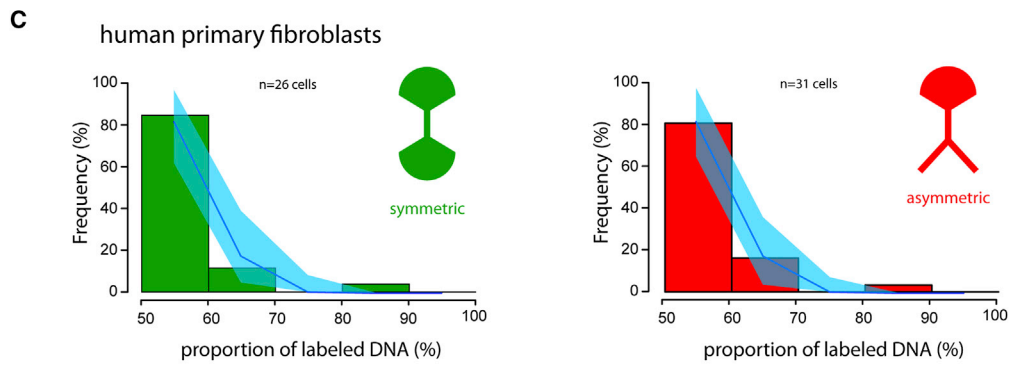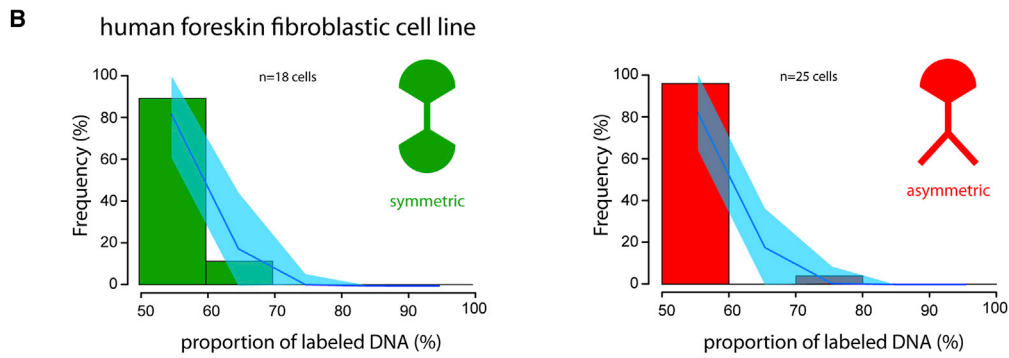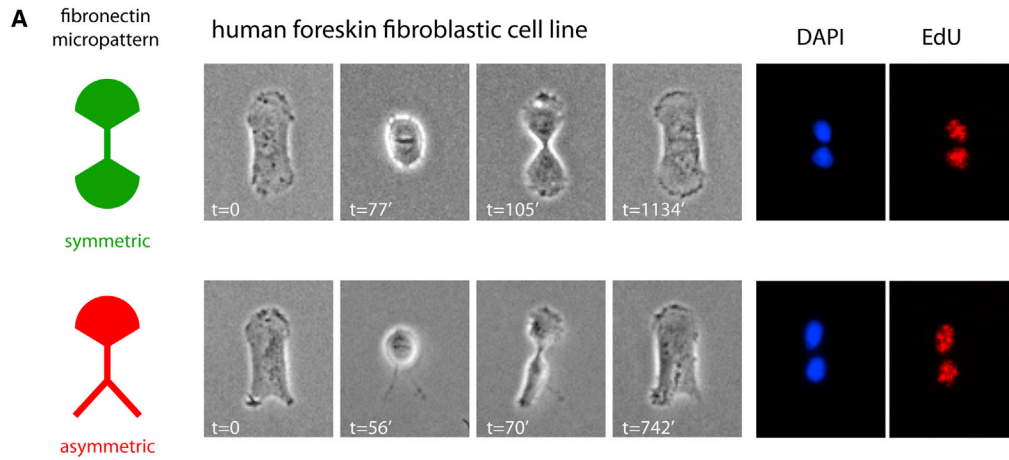
(B) Estimation of the mean and SD of the proportion of divided hMSCs displaying biased DNA segregation using a bootstrap method based on data shown in Figure 2C. The mean frequency of biased DNA segregation was a significantly higher (t test) for divided cells on asymmetric micropatterns than on symmetric micropatterns.

(C) Histograms of the observed frequencies for DNA segregation rates (in 10% intervals) shown in Figure 2C overlaid with line graphs describing the numerical simulation of DNA segregation rates of random chromatid segregation in the same number of cells (see Supplemental Experimental Procedures). Light blue areas indicate the 99% confidence intervals. Note that the part of the observed distribution (red bars, right histogram) on asymmetric micropatterns is not compatible with the random process.

micropatterns, biased DNA segregation was observed in 14 out of 43 divided cells. Bootstrapping methods have been developed to estimate the confidence interval of data set with "not-quite large samples" (Tukey, 1958; Davison, 1997). They are based on resampling with replacements of the actual data set keeping the number of observations constant. These new data can then be used to estimate the actual mean and SD of the few measurements. We used a bootstrapping method to compare the frequencies of biased DNA segregation in cells plated on symmetric and asymmetric micropatterns (Figure 3B). It appeared that the estimated difference between cells on sym-

metric and asymmetric micropatterns (6% and 33%, respectively) was highly significant (p = 0.00035).

The prominent segregation bias in cells plated on asymmetric micropatterns was also highlighted by the direct comparison between the observed distribution of DNA segregation rates with the numerical simulation of random segregation (Figure 3C) (see Methods in Supplemental Information) (Falconer et al., 2010). On symmetric micropatterns, almost all DNA segregation measurements were within the 99% CI defined by random segregation, whereas on asymmetric micropatterns, the bias DNA segregation measurements appeared as a distinct

A fibronectin micropattern / human foreskin fibroblastic cell line / DAPI / EdU

symmetric
t=0   t=77′   t=105′   t=1134′

asymmetric
t=0   t=56′   t=70′   t=742′

B human foreskin fibroblastic cell line

n=18 cells — symmetric
n=25 cells — asymmetric

(Frequency (%) vs proportion of labeled DNA (%))

C human primary fibroblasts

n=26 cells — symmetric
n=31 cells — asymmetric

(Frequency (%) vs proportion of labeled DNA (%))

D human foreskin fibroblastic cell line / human primary fibroblasts

p = 0.49   p = 0.21

Proportion of labeled DNA (%)

First mitosis   Second mitosis   Second mitosis

E

p = 0.00037   p = 0.00008

Frequency of biased DNA segregation (%)

mesenchymal stem cells   fibroblastic cell line   primary fibroblasts

(legend on next page)

(secondary) distribution (Figure 3C). These analyses confirmed the existence of a nonrandom mechanism directing chromosome segregation in hMSCs in response to asymmetric extracellular signals associated with cell adhesion.

We then examined the cells displaying asymmetric DNA segregation ratios to identify whether the labeled, chromatids were preferentially segregated in the daughter cell positioned on the more-adhesive or less-adhesive side of the micropattern. However, cells were generally fixed and labeled several hours after division, during which time they could have repositioned with respect to the micropattern geometry. Moreover, it was difficult to retrospectively identify from the video recordings the original position of the nonlabeled cells immediately after they emerged from cell division. Nevertheless, in four out of the five videos in which this analysis was feasible, the labeled chromatids were segregated in the daughter cell located on the less adhesive side of the micropattern (as illustrated in Figure 2B). This supported the existence of a correlation between the greater concentration of localized cell adhesions at one part of the cell and the directed segregation of older chromatids toward this part (Tajbakhsh and Gonzalez, 2009).

Cell Adhesion Asymmetry Had No Effect on DNA Segregation in Normal Fibroblasts

To test whether the role of adhesion asymmetry on biased DNA segregation was specific to stem cells, we performed the same EdU segregation test on BJ1, a normal human foreskin fibroblast cell line (Figure 4A). Asymmetric DNA segregation ratios were observed but were infrequent and largely consistent with random chromatid segregation (Figure 4B). Similar distributions of DNA segregation rates were observed in fibroblasts derived from the skin of two healthy donors (Figure 4C). In addition, no difference in the frequency distributions of different DNA segregation ratios could be detected between cells plated on symmetric and asymmetric micropatterns for both type of fibroblasts (Figure 4D; Wilcoxon test). Biased DNA segregation was observed in 1/26 divided primary fibroblast cell on symmetric micropatterns and in two divided cells on asymmetric micropatterns (1/25 in BJ1, 1/31 in primary fibroblasts). However, the frequencies of biased segregation on symmetric micropatterns were significantly lower than in hMSCs (14/43) (Figure 4E).

DISCUSSION

Together, these results have led us to the formulation of two important conclusions: the spatial distribution of cell adhesion is a major parameter in the regulation of biased DNA segregation, and mesenchymal stem cells are more sensitive to this parameter than fibroblasts.

It should first be noted that this study extends the previous observations of biased DNA segregation previously made in mouse stem cells and transformed, or immortalized, human cell lines to human primary stem cells. Our work on human cells was motivated by the interest this extension constitutes for basic research and potential therapeutic applications.

However, there were two main limitations to the experimental procedures used in this study. Cells had to be cultured in vitro. Individual cell proliferation was infrequent and variable. In addition, EdU staining is less precise than counting labeled chromosomes to evaluate a bias in chromatid segregation (Falconer et al., 2010; Sauer et al., 2013). Nevertheless, the relatively low numbers of measurements were obtained from four different donors and analyzed with three distinct statistical tests, all of which validate the significance of the observed differences.

In the following paragraphs, we discuss the conditions in which these experiments were performed as well as their biological relevance and physiological implications.

Cell Adhesion and Tissue Geometry

Cell culture on ECM-coated micropatterns obviously does not mimic the actual in situ conditions, but it does offer the potential to manipulate the spatial distribution of cell adhesions and thereby the potential to provide mechanistic insights to cell behavior in vivo (Morin and Bellaïche, 2011). The geometries of the micropatterns in this study probably have no exact counterparts in tissues. However, in many tissues, cells encounter irregular patterns of adhesion contacts. This is notably the case in the highly structured and heterogeneous niches in which stem cells are confined (Ellis and Tanentzapf, 2010; Marthiens et al., 2010; Brizzi et al., 2012). Our results suggest that in these conditions, a local clustering of adhesion in one part of the cell could trigger biased DNA segregation.

Biased DNA segregation also occurred at low frequency in divided hMSCs on symmetric adhesion patterns. This may be in accordance with the absence of clear biased segregation in hematopoietic stem cells (Kiel et al., 2007) where the weak adhesion of hematopoietic stem cells may not be sufficient to stimulate biased DNA segregation. But this does not exclude the possibility that in defined conditions hematopoietic stem cells could transiently develop asymmetric adhesion contacts (Ehninger and Trumpp, 2011) and then have the potential to promote biased DNA segregation. Hence, stem cells have a mechanism supporting bias DNA segregation that operates at a basal level in all conditions but is selectively amplified when stem cells form asymmetric adhesion contacts.

Figure 4. Quantification of DNA Segregation in Fibroblasts

(A) BJ1 cells were plated on symmetric (upper panel) and asymmetric (lower panel) fibronectin micropatterns, and examined as described in Figure 2B.

(B and C) Histograms of the frequencies for DNA segregation rates (in 10% intervals) of (B) BJ1 cells or (C) human primary fibroblasts when plated on symmetric (left) and asymmetric (right) micropatterns, overlaid with numerical simulations of ratios expected from random chromatid segregation in the same number of cells (see Supplemental Experimental Procedures). Light blue areas indicate the 99% confidence interval.

(D) Box plot representations DNA segregation rates after the first and the second division on symmetric and asymmetric micropatterns for BJ1 and primary fibroblast. The frequencies of asymmetric DNA segregation rates (those superior to the threshold of 55% shown by the blue dotted line) were compared with a Wilcoxon test, which revealed no significant difference between DNA segregation on symmetric and asymmetric micropatterns.

(E) Estimation of the mean and SD of the proportion of divided BJ1 or primary fibroblasts displaying biased DNA segregation using a bootstrap method. On asymmetric micropatterns, the mean frequency of biased DNA segregation was a significantly higher (t test) for divided hMSCs than for BJ1 or primary fibroblasts.

Notably, stem cells can develop anisotropic interactions with the ECM and with neighboring cells (Marthiens et al., 2010; Chen et al., 2013). Whether the regulation of DNA segregation by the geometry of the ECM we described here also applies to the geometry of cell-cell interactions remains to be investigated. Considering the shared characteristics in the mechanism of spindle orientation by cell-matrix and cell-cell adhesions (Morin and Bellaïche, 2011), it would not be surprising to observe similarities in the regulation of DNA segregation. Indeed variations of the density of cell-cell contacts in culture have been shown to affect asymmetric DNA segregation ratios (Pine et al., 2010).

Interestingly, the role of cell adhesion symmetry suggests that biased DNA segregation is promoted along the boundaries of a tissue, but not within internal aspects of the tissue. The symmetrical environment cells encounter within the tissue stroma may inhibit biased DNA segregation, whereas at the tissue periphery, interfaces between cell types with distinct adhesion properties, and frontiers between distinct organs, may be particularly suited to promote it. All boundaries may not be capable to induce biased DNA segregation, but the asymmetry they constitute may be a required condition. Interestingly, tissue boundaries are the preferential location of stem cells. Do stem cells move toward tissue boundaries, or do the physical properties of boundaries activate stem cell traits? This is an interesting debate in which the specific activation of biased DNA segregation at the tissue boundary could be also considered.

Proportions of Asymmetric DNA Segregation

Although we clearly identified a bias in DNA strand segregation, the segregation of all labeled strands in one of the daughter cells, as it has been described in muscle stem cells (Conboy et al., 2007; Rocheteau et al., 2012), was rarely observed (1/43 in hMSCs plated on asymmetric micropatterns). This could be a consequence of working with primary cells in vitro. Indeed, the proportion of asymmetric DNA segregation in muscle stem cells is also lower when the cells are maintained in culture (Conboy et al., 2007; Rocheteau et al., 2012; Shinin et al., 2006). In addition, we followed the procedure recommended by the European Group for Blood and Marrow Transplantation to isolate hMSCs (Le Blanc et al., 2008). The selection process is based on differential cell adhesion and did not include any further immunosorting step. So the population of hMSCs we used was probably heterogeneous and may have contained some differentiated cells in which biased DNA segregation is less active.

Indeed, biased DNA segregation was observed at low frequencies in fibroblasts. It could be due to the presence of few stem cells in the population or to a vestigial mechanism in differentiated cells. Both hypotheses suggest that the capacity to bias DNA segregation is progressively lost as cells differentiate.

Considered together, the reduction of biased DNA segregation in stem cells during cell culture and during cell differentiation suggests that the cell's capacity to bias DNA segregation is not an on-off process but is subject to a graded regulation. Depending on the cell's capacity, the degree of the DNA segregation bias would reflect the degree of external asymmetry.

How the capacity to bias DNA segregation is coupled to cell differentiation state is an interesting question. One hypothesis is that this capacity is related to the regulation of cytoskeleton polarization. Interestingly, cytoskeleton polarization is not an on-off process either, and the well-known intrinsic polarization capacities of the actin cytoskeleton by symmetry break (Mullins, 2010) can be modulated and stabilized by additional microtubule-associated signaling pathways (Wang et al., 2013). Whether similar pathways are coregulated with stemness pathways and render the stem cell cytoskeleton more responsive to external changes is an exciting hypothesis. Another nonexclusive hypothesis is that the capacity is acquired by prolonged exposure to environmental asymmetries. Stem cells at tissue boundaries are permanently exposed to asymmetric conditions and thereby may become more activated and responsive than fibroblasts in the stroma, which are exposed to symmetric conditions. When stem cells are removed from their niche and placed in a relatively homogeneous environment in culture, they suddenly become exposed to symmetric conditions and start losing their capacity to undergo biased DNA segregation. In accordance with such a mechanism, the level of activation would not be directly related to stemness but to a progressive adaptation to the degree of symmetry in the cell's microenvironment.

The two points we discussed above, the spatial regulation associated with tissue boundaries and the temporal regulation of the level of activation allowing cells to respond to external asymmetry, offer insights into the regulation of biased DNA segregation. The capacity of a cell to bias DNA segregation may not be predetermined, but it may be reprogrammable. Therefore, microenvironment geometry could dynamically modulate cell responsiveness and the degree of biased DNA segregation. Accordingly, the alteration of the cell's position within the tissue, during development, tissue renewal, or malignant transformation, would affect the cell's capacity to bias DNA segregation. In addition, sudden changes in cell microenvironment geometry, like tissue injury, would rapidly modulate the cell's activation level and trigger biased DNA segregation. This hypothesis is consistent with the observation that muscle stem cells undergo biased DNA segregation upon muscle injury only. It suggests that stem cells, like hair follicle stem cells (Sotiropoulou et al., 2008) or intestinal epithelial stem cells (Escobar et al., 2011), may not bias DNA segregation in normal conditions but could do so punctually in response to local tissue changes such as a wound, an inflammation, or a local variation of cell density. Thus, the dynamic regulation of biased DNA segregation by local asymmetries would be proficient for tissue repair after wounding and for proper tissue homeostasis in rapidly growing tissue during development.

EXPERIMENTAL PROCEDURES

Bone Marrow Samples

Bone marrow (BM) samples were harvested from washed filters used during BM graft processing for allogeneic BM transplantation. All samples were taken after receiving informed consent according to approved institutional guidelines (Assistance Publique, Hôpitaux de Paris, Paris, France).

hMSC Culture and Characterization

BM hMSCs were isolated and expanded as previously described (Arnulf et al., 2007). Briefly, healthy donor BM cells were cultured at the initial density of 5.10^4 cells/cm^2 in Minimum Essential Medium-α (Invitrogen), supplemented

with 10% fetal bovine serum (HyClone), Glutamax-I (2 mM; Invitrogen), basic fibroblast growth factor (1 ng/mL; R&D Systems), and antibiotic/antimycotic (1%, Invitrogen). After 24–48 hr, nonadherent cells were removed and medium was changed. Adherent cells were then trypsinized, harvested, and cultured by seeding 5.10^3 cells/cm^2. Cultures were fed every 2 to 3 days and trypsinized every 5 days. In all experiments, hMSCs were used at passage 3 to 4.

Monoclonal antibodies conjugated with either fluorescein isothiocyanate or phycoerythrin and directed to CD34, CD45, CD73, CD90, CD13, CD29, CD105, or matched isotype control (all purchased from Becton Dickinson, Le Pont de Claix, France) were used for hMSC immunophenotyping according to the manufacturer's protocol. Data were acquired and analyzed on a five-parameter flow cytometer (FACScalibur, Becton Dickinson) with CellQuestPro software (Becton Dickinson). In accordance with the literature, the BM hMSCs used in our study did not express hematopoietic antigens, such as CD14, CD34, and CD45, and were found positive for CD73, CD90, CD29, CD44, and CD105 expression.

Fibroblast Culture
Primary cultures of dermal fibroblasts were derived from skin biopsy specimens obtained during mammoplasty surgery. All samples were taken after receiving informed consent according to approved institutional guidelines (Assistance Publique, Hôpitaux de Paris, Paris, France). Cells were cultured in Dulbecco's modified Eagle's medium containing 10% fetal bovine serum (HyClone), 100 U/ml penicillin, and 1 mg/ml streptomycin. Fibroblasts were used between the third and fourth passages.

Human foreskin fibroblast BJ1 (ATCC) cells were cultured in Minimum Essential Medium-α (Invitrogen), supplemented with 10% fetal bovine serum (HyClone), Glutamax-I (2mM; Invitrogen), nonessential amino acid (1x; Invitrogen), and 100 U/ml penicillin, 100 μg/ml streptomycin (Invitrogen).

Both cell types were cultured in a humidified incubator at 37°C with 5% CO_2 atmosphere.

Micropatterns
Micropatterns coated with native and Alexa 650-labeled fibronectin were purchased from Cytoo. They were fabricated on thin (170-μm-thick) glass slides compatible with fluorescence imaging and video recording.

SUPPLEMENTAL INFORMATION

Supplemental Information includes Supplemental Experimental Procedures and four figures and can be found with this article online at http://dx.doi.org/10.1016/j.celrep.2013.09.019.

REFERENCES

Arnulf, B., Lecourt, S., Soulier, J., Ternaux, B., Lacassagne, M.-N., Crinquette, A., Dessoly, J., Sciaini, A.-K., Benbunan, M., Chomienne, C., et al. (2007). Phenotypic and functional characterization of bone marrow mesenchymal stem cells derived from patients with multiple myeloma. Leukemia 21, 158–163.

Brizzi, M.F., Tarone, G., and Defilippi, P. (2012). Extracellular matrix, integrins, and growth factors as tailors of the stem cell niche. Curr. Opin. Cell Biol. 24, 645–651.

Chen, S., Lewallen, M., and Xie, T. (2013). Adhesion in the stem cell niche: biological roles and regulation. Development 140, 255–265.

Conboy, M.J., Karasov, A.O., and Rando, T.A. (2007). High incidence of non-random template strand segregation and asymmetric fate determination in dividing stem cells and their progeny. PLoS Biol. 5, e102.

Davison, A.C. (1997). Bootstrap Methods and Their Application (Cambridge: Cambridge University Press).

Ehninger, A., and Trumpp, A. (2011). The bone marrow stem cell niche grows up: mesenchymal stem cells and macrophages move in. J. Exp. Med. 208, 421–428.

Ellis, S.J., and Tanentzapf, G. (2010). Integrin-mediated adhesion and stem-cell-niche interactions. Cell Tissue Res. 339, 121–130.

Escobar, M., Nicolas, P., Sangar, F., Laurent-Chabalier, S., Clair, P., Joubert, D., Jay, P., and Legraverend, C. (2011). Intestinal epithelial stem cells do not protect their genome by asymmetric chromosome segregation. Nat. Commun. 2, 258.

Evano, B., and Tajbakhsh, S. (2013). Sorting DNA with asymmetry: a new player in gene regulation? Chromosome Res. 21, 225–242.

Falconer, E., Chavez, E.A., Henderson, A., Poon, S.S., McKinney, S., Brown, L., Huntsman, D.G., and Lansdorp, P.M. (2010). Identification of sister chromatids by DNA template strand sequences. Nature 463, 93–97.

Gönczy, P. (2008). Mechanisms of asymmetric cell division: flies and worms pave the way. Nat. Rev. Mol. Cell Biol. 9, 355–366.

Guilak, F., Cohen, D.M., Estes, B.T., Gimble, J.M., Liedtke, W., and Chen, C.S. (2009). Control of stem cell fate by physical interactions with the extracellular matrix. Cell Stem Cell 5, 17–26.

Inaba, M., and Yamashita, Y.M. (2012). Asymmetric stem cell division: precision for robustness. Cell Stem Cell 11, 461–469.

Kajstura, J., Bai, Y., Cappetta, D., Kim, J., Arranto, C., Sanada, F., D'Amario, D., Matsuda, A., Bardelli, S., Ferreira-Martins, J., et al. (2012). Tracking chromatid segregation to identify human cardiac stem cells that regenerate extensively the infarcted myocardium. Circ. Res. 111, 894–906.

Karpowicz, P., Morshead, C., Kam, A., Jervis, E., Ramunas, J., Cheng, V., van der Kooy, D., and van der Kooy, D. (2005). Support for the immortal strand hypothesis: neural stem cells partition DNA asymmetrically in vitro. J. Cell Biol. 170, 721–732.

Kiel, M.J., He, S., Ashkenazi, R., Gentry, S.N., Teta, M., Kushner, J.A., Jackson, T.L., and Morrison, S.J. (2007). Haematopoietic stem cells do not asymmetrically segregate chromosomes or retain BrdU. Nature 449, 238–242.

Le Blanc, K., Frassoni, F., Ball, L., Locatelli, F., Roelofs, H., Lewis, I., Lanino, E., Sundberg, B., Bernardo, M.E., Remberger, M., et al. (2008). Mesenchymal stem cells for treatment of steroid-resistant, severe, acute graft-versus-host disease: a phase II study. Lancet 371, 1579–1586.

Li, R., and Gundersen, G.G. (2008). Beyond polymer polarity: how the cytoskeleton builds a polarized cell. Nat. Rev. Mol. Cell Biol. 9, 860–873.

Maiato, H., and Barral, Y. (2013). Unbiased about chromosome segregation: give me a mechanism and I will make you "immortal". Chromosome Res. 21, 189–191.

Marthiens, V., Kazanis, I., Moss, L., Long, K., and Ffrench-Constant, C. (2010). Adhesion molecules in the stem cell niche—more than just staying in shape? J. Cell Sci. 123, 1613–1622.

Merok, J.R., Lansita, J.A., Tunstead, J.R., and Sherley, J.L. (2002). Cosegregation of chromosomes containing immortal DNA strands in cells that cycle with asymmetric stem cell kinetics. Cancer Res. 62, 6791–6795.

Morin, X., and Bellaïche, Y. (2011). Mitotic spindle orientation in asymmetric and symmetric cell divisions during animal development. Dev. Cell 21, 102–119.

Mullins, R.D. (2010). Cytoskeletal mechanisms for breaking cellular symmetry. Cold Spring Harb. Perspect. Biol. 2, a003392.

Pine, S.R., Ryan, B.M., Varticovski, L., Robles, A.I., and Harris, C.C. (2010). Microenvironmental modulation of asymmetric cell division in human lung cancer cells. Proc. Natl. Acad. Sci. USA 107, 2195–2200.

Potten, C.S., Owen, G., and Booth, D. (2002). Intestinal stem cells protect their genome by selective segregation of template DNA strands. J. Cell Sci. *115*, 2381–2388.

Rocheteau, P., Gayraud-Morel, B., Siegl-Cachedenier, I., Blasco, M.A., and Tajbakhsh, S. (2012). A subpopulation of adult skeletal muscle stem cells retains all template DNA strands after cell division. Cell *148*, 112–125.

Rozario, T., and DeSimone, D.W. (2010). The extracellular matrix in development and morphogenesis: a dynamic view. Dev. Biol. *341*, 126–140.

Sauer, S., Burkett, S.S., Lewandoski, M., and Klar, A.J.S. (2013). A CO-FISH assay to assess sister chromatid segregation patterns in mitosis of mouse embryonic stem cells. Chromosome Res. *21*, 311–328.

Shinin, V., Gayraud-Morel, B., Gomès, D., and Tajbakhsh, S. (2006). Asymmetric division and cosegregation of template DNA strands in adult muscle satellite cells. Nat. Cell Biol. *8*, 677–687.

Smith, G.H. (2005). Label-retaining epithelial cells in mouse mammary gland divide asymmetrically and retain their template DNA strands. Development *132*, 681–687.

Sotiropoulou, P.A., Candi, A., and Blanpain, C. (2008). The majority of multipotent epidermal stem cells do not protect their genome by asymmetrical chromosome segregation. Stem Cells *26*, 2964–2973.

Tajbakhsh, S., and Gonzalez, C. (2009). Biased segregation of DNA and centrosomes: moving together or drifting apart? Nat. Rev. Mol. Cell Biol. *10*, 804–810.

Théry, M., Racine, V., Pépin, A., Piel, M., Chen, Y., Sibarita, J.-B., and Bornens, M. (2005). The extracellular matrix guides the orientation of the cell division axis. Nat. Cell Biol. *7*, 947–953.

Théry, M., Jiménez-Dalmaroni, A., Racine, V., Bornens, M., and Jülicher, F. (2007). Experimental and theoretical study of mitotic spindle orientation. Nature *447*, 493–496.

Tukey, J.W. (1958). Bias and confidence in not quite large samples. Ann. Math. Stat. *29*, 614.

Wang, Y., Ku, C.-J., Zhang, E.R., Artyukhin, A.B., Weiner, O.D., Wu, L.F., and Altschuler, S.J. (2013). Identifying network motifs that buffer front-to-back signaling in polarized neutrophils. Cell Rep. *3*, 1607–1616.

Yamashita, Y.M. (2010). Cell adhesion in regulation of asymmetric stem cell division. Curr. Opin. Cell Biol. *22*, 605–610.